

STRESS ANALYSIS AND STRENGTH EVALUATION OF SCARF ADHESIVE

JOINTS SUBJECTED TO STATIC TENSILE LOADINGS

HE Dan Prof. Toshiyuki SAWA* Takeshi IWAMOTO Yuya HIRAYAMA

Graduate School of Mechanical Engineering

Hiroshima University

1-4-1 Kagamiyama, Higashihiroshimashi, Hiroshima, 739-8527, Japan

*To whom correspondence should be addressed. Tel:+81-82-424-7577

Fax: +81-82-424-7577 Email address: Sawa@mec.hiroshima-u.ac.jp

ABSTRACT

The stress distributions in scarf adhesive joints under static tensile loadings are analyzed using three-dimensional finite-element calculations. The effects of adhesive Young's modulus, adhesive thickness and scarf angle in the adherend on the interface stress distributions are examined. As the results, it is found that the maximum value of the maximum principal stress occurs at the edge of the interfaces. The differences in the interface stress distributions between the 2-D and the 3-D FEM results are demonstrated. It is also observed from the 3-D FEM results that the maximum value of the maximum principal stress is the smallest when the scarf angle is around 60 degree, while it is around 52 degree in the 2-D FEM when the singular stress at the edges vanishes. In addition, the joint strength is estimated using the interface stress distribution obtained from the FEM calculations. For verification of the FEM calculations, experiments were carried out to measure the strengths and the strains in the joints under static tensile loadings using strain gauges. Fairly good agreements were observed between the 3-D FEM and the measured results for strains. Therefore, for the joint strength, the results remain conservative.

Keywords: Stress analysis; Interface stress distribution; Singular stress; FEM; Adhesive; Tension; Joint strength; Scarf adhesive joint

1. INTRODUCTION

Recently, as the adhesive performance has enhanced, adhesive joints have been used in a large variety of industries such as mechanical structure, automobile, aerospace engineering, wood industry and so on. However, large variation in joint strength occurs in the adhesive joints, so it is necessary and important to research on the stress distributions and strength evaluation in the adhesive joints under several types of external loadings. So far, a lot of studies have been performed on the stress analysis for butt adhesive joints and lap joints^{[1]-[11]}. Also some studies^{[12]-[23]} on the stress analysis for scarf joints have been reported. But no report about the effects of geometrical (e.g. the scarf angle, the adhesive thickness) and material parameters (e.g. the Young's modulus of adhesive) on the stress distributions in scarf joints has been carried out with both two-dimensional (2-D) and three-dimensional (3-D) FEM calculations. In designing scarf adhesive joints, an important issue is how to determine the scarf angle, the adhesive material properties and the adhesive thickness from a mechanical engineering standpoint. Thus, it is necessary to examine the effect of the scarf angle, the adhesive material properties and the adhesive thickness on the interface stress distributions in the joints and the joint strengths.

In this paper, the stress distributions in scarf adhesive joints of similar adherends under static tensile loadings are analyzed using both the 2-D and the 3-D finite-element method (FEM). The FEM code employed was ANSYS. The results of the interface

stress distributions were compared between the 2-D and the 3-D FEM calculations. The effects of scarf angle, adhesive Young's modulus and adhesive thickness were examined on the interface stress distributions. For verification of the 3-D FEM calculations, the strains in the joints were measured and the results were compared with those obtained from the 3-D FEM calculations. The joint strengths are estimated using the obtained interface stress distributions in elasto-plastic deformation range. Experiments under the same condition as the FEM calculations were also carried out to measure the strengths of the scarf joints subjected to the tensile loads. The numerical results were compared with the experimental ones.

2. FEM CALCULATIONS FOR THE INTERFACE STRESS

Figure 1 shows a model for the 3-D FEM calculations of scarf adhesive joints. The upper and lower adherends have the same dimensions and materials, and are subjected to static tensile loadings. Young's modulus and Poisson's ratio of the adherends are denoted by E_1 and ν_1 , those of the adhesive by E_2 and ν_2 . The adherend length is denoted by h_1 (see Fig.1), the adherend width and thickness by w and $2t_1$, respectively. The adhesive length and thickness are denoted by $2l$, and $2t_n$, respectively. Half part of the joint is analyzed because the joint is symmetric with respect to $z=t_1$. The origins of x - y - z and s - n coordinate systems are at the same position which is denoted by 0 (see Fig.1). The boundary conditions applied are as follows: The lower adherend is fixed in the y -direction and the tensile loading is applied to the end of the upper adherend.

Figure 2(a) shows an example of mesh divisions of a scarf adhesive joint in the 2-D FEM calculations. The FEM code employed was ANSYS. The total number of nodes and elements were 1891 and 1800, respectively. The smallest element size was $5 \times 5 \mu\text{m}$ at the interfaces between the adhesive and the adherends. Figure 2(b) shows an example of mesh divisions of the scarf adhesive joint in the 3-D FEM calculations. The total number of nodes was chosen as 30256 and the total number of elements as 27000. The smallest element size was chosen as $5 \times 5 \times 5 \mu\text{m}$ at the interfaces. SS400 (JIS) mild steel was chosen as the adherend material and epoxy (SUMITOMO 3M Co., Ltd., Scotch-Weld 1838) as the adhesive. In the FEM calculations, bi-linear material models were employed for simulating the nonlinear constitutive relation for the adhesive and adherend materials (See the dotted line in Fig. 4).

3. EXPERIMENTAL METHOD

Figure 3 shows the dimensions of the adherend used in the experiments for measuring the strains in the adherends and the joint strengths. The specimens were designed and fabricated such that the bonding area of each specimen holds constant at 288 mm^2 . Table 1 shows the scarf angles and the corresponding adherend widths. The thickness of the specimen was chosen as 9 mm. The adhesive thickness was 0.1 mm. The material of the specimens was chosen as mild steel (SS400, JIS). The experiments were carried out after bonding and solidifying a pair of specimens for eight hours with an epoxy (SUMITOMO 3M Co., Ltd., Scotch-Weld 1838) at 60°C .

Figure 4 shows the stress-strain relationship of the adhesive material used in the experiments. The solid line indicates the experimentally measured result and the dotted line indicates the bi-linear model employed in the FEM calculations. The rupture stress of the adhesive material is measured as 50.96Mpa, which can be seen in Fig.4.

Figure 5 shows the schematics of the experimental setup for measuring strains and joint strengths under tensile loadings. A compression which was applied to the test jigs was converted to a tensile loading in the experimental setup shown in Fig.5. In the experiments, strains at 3 points at the adhesive layer were measured by strain gauges with a length of 1 mm (KYOWA Electronic Instruments Co., Ltd., KFC-C1-1 1), and the magnitude of the applied load was measured with a load cell. The output signals were recorded by an oscilloscope through dynamic amplifiers. The rupture loads were also measured.

4. NUMERICAL RESULTS AND COMPARISONS WITH EXPERIMENTS

4.1. Results of FEM Calculations

4.1.1. Effect of scarf angle of the adherend on the stress distribution in case of the 2-D FEM calculations

The 2-D FEM calculations were done for the scarf adhesive joint shown in Fig.1. As the singular stresses occur at the adhesive-adherend interfaces and they are essential in the determination of joint strength, the stress distributions at the interfaces have been mainly examined. Figure 6(a) shows the effect of the scarf angle on the interface stress

distribution near the left edge obtained from the 2-D FEM calculations. Figure 6(b) shows the effect of the scarf angle on the interface stress distribution near the right edge obtained from the 2-D FEM calculations. In Fig.6, the ordinate indicates the ratio of the maximum principal stress σ_1 to the average stress σ_0 due to the applied tensile loading shown in Fig.1. The abscissa indicates the coordinate s divided by the length of the adhesive layer l . From the results, it is found that the singular stress occurs at the edge of the interfaces and the maximum value of the maximum principal stress σ_1 occurs at the edge of the interfaces. It is also found that the singular stress is maximum for a scarf angle of 90° (butt joint) and it vanishes at a scarf angle of 51.86° [10]. Consequently, the joint strength is assumed to be maximum when the scarf angle is 51.86° , while it is minimum at the scarf angle of 90° (butt joint). Also, it is found that, when the scarf angle increases from 51.86° , the singular stress occurs at the right sides of both the upper and lower interfaces and it occurs at the left sides of both the upper and lower interfaces when the scarf angle decreases from 51.86° .

4.1.2. Effect of scarf angle of the adherend on the interface stress distribution in the 3-D FEM calculations

Figure 7(a) shows the effect of the scarf angle on the interface stress distribution near the left edge of the interfaces obtained from the 3-D FEM calculations. Figure 7(b) shows the effect near the right edge of the interface. From the results, it is found that the singular stress occurs at the edge of the interfaces and the maximum value of the

maximum principal stress σ_1 occurs at the edge of the interfaces. It is also observed that the singular stress is the maximum at a scarf angle of 45° and it is the minimum at a scarf angle of 60° . Consequently, the joint strength is assumed to be maximum when the scarf angle is 60° , while it is minimum at the scarf angle of 45° . The case where the scarf angle was around 51.86° was also calculated. However, in the 3-D FEM calculations, it can not be observed that the singular stress vanishes when the scarf angle is around 51.86° . The results obtained from the 3-D FEM calculation are so different from those obtained from the 2-D FEM calculation.

Figure 8 shows the interface stress distribution in the adherend thickness direction (in the z direction shown in the figure) obtained from 3-D FEM calculation where $s=-l$ and $n=0$. It is seen that the singular stress occurs near the edge of the interfaces in the z -direction.

4.1.3 Effect of adhesive Young's modulus on the interface stress distributions

Figure 9 shows the effect of adhesive Young's modulus E_2 on the interface stress distribution along the s -axis of the scarf joints with a scarf angle of 60° obtained from the 3-D FEM calculations, where Young's modulus E_2 is varied as 1.67 GPa, 3.34 GPa and 6.68 GPa. It is found that the maximum principal stress in the singular region ($-1.0 < s/l < -0.95, z=t_2/2$) increases as the value of E_2 decreases. As the result, it is assumed that the joint strength decreases as the value of E_2 decreases while the adherend Young's modulus E_1 is held constant at 209 GPa. This is an obvious result

since stress is always reduced as the material properties become similar.

4.1.4 Effect of adhesive thickness on the interface stress distributions

Figure 10 shows the effect of the adhesive thickness $2t_n$ on the interface stress distributions along the s -axis of the scarf joints with a scarf angle of 60° obtained from the 3-D FEM calculations. The adhesive thickness $2t_n$ was chosen as 0.05 mm, 0.1 mm and 0.15 mm. It is shown that the maximum principal stress in the singular region ($-1.0 < s/l < -0.95, z = t_2/2$) increases as the adhesive thickness $2t_n$ increases. As a result, it is assumed that the joint strength increases as the adhesive thickness $2t_n$ decreases.

4.2 COMPARISON OF THE STRAINS BETWEEN THE FEM RESULTS AND THE EXPERIMENTAL RESULTS

Figure 11 shows the comparison of the strains between the 3-D FEM results and the experimental results in the scarf adhesive joint subjected to the static tensile loading. The ordinate is the strain ε_y in the y -direction. The abscissa is the location. The black circle symbols \bullet show the measured results. The configuration of the scarf joint used for comparison of strains is as follows. The scarf angle is 60° . The material constants of adherends, E_1 and ν_1 , are 209 GPa and 0.29, respectively. The material constants of the adhesive layer, E_2 and ν_2 , are 3.34 GPa and 0.38, respectively. The adhesive thickness is chosen as 0.1 mm. In the experiments, the strain (ε_y) was measured at three positions along adhesive layer (as shown in Fig.11), while in the 3-D FEM calculation, the values of ε_y were averaged at the corresponding areas of the glued strain gauge along the

adhesive layer. The solid line shows the 3-D FEM result. It is found that the 3-D FEM result of the strain is well consistent with the experimental results.

4.3 JOINT STRENGTH

In this study, the value of the exerted tensile stress when the singular maximum principle stress in the joint reaches the rupture strength of the adhesive is determined as the rupture stress. The joint strength was prospected in this way with the 3-D FEM calculations for several scarf joints with different scarf angles. Then, the experiments to measure the joint strength (the rupture stress) were done for the scarf joints. Figure 12 shows the joint strengths obtained from the stress due to the 3-D FEM calculations and from the experiments. For each scarf angle, 20 specimens were tested. The scatter in the strength is shown in Fig.12 with a vertical line. While the averaged value of the joint strength for each scarf angle is denoted by the symbol ●. The symbol □ represents the values of joint strength obtained from the 3-D FEM calculations due to the maximum principle stress failure criteria. It is seen that the values of the joint strength obtained from the 3-D FEM calculations are a little bit conservative with those measured by the experiments. However, the joint strengths can be estimated more safely by the FEM calculations.

5. CONCLUSIONS

In this paper, the interface stress distributions in scarf adhesive joints subjected to static tensile loadings were calculated by the two-dimensional and the three-dimensional

FEM and the joint strengths were estimated using the obtained interface stress distributions. In addition, the effects of some factors were examined on the interface stress distributions. The following results were obtained.

1. The effect of scarf angle of the adherend on the interfaces stress distribution was compared between the two-dimensional and the three-dimensional FEM calculations. The results show that the singular stress vanishes at a scarf angle of about 52 degrees in the two-dimensional FEM calculations, however it doesn't vanish when the scarf angle is about 52 degree in the three-dimensional FEM calculations. In addition, the maximum value of the maximum principal stress σ_I is the smallest for the present joint when the scarf angle is 60 degree in the 3-D FEM calculation. So it is assumed that the joint strength is maximum for a scarf angle of approximately 60 degree.

2. The effects of Young's modulus of the adhesive, the thickness of the adhesive layer on the interface stress distribution were examined using the 3-D FEM. The results show that the singular stress at the edge of the interface decreases as the adhesive Young's modulus increases and as the adhesive thickness decreases.

3. From the 3-D FEM results, it was found that the singular stress occurred at the edges of the interfaces in the thickness direction as well as at the edge of the interfaces in the width direction. Thus, the singular stress obtained from the 3-D FEM was larger than that obtained from the 2-D FEM.

4. The experiments to measure the strains and the joints strengths were carried out for

verification of the FEM calculations. The 3-D FEM results were well consistent with the experimental ones.

5. The joint strength was estimated using the interface stress distributions obtained from the 3-D FEM calculations. The estimated joint strengths were conservative with the experimental results. It was found that the rupture stress was maximum when the scarf angle was around 60 degree in the present scarf adhesive joints.

6. REFERRNCES

- [1] R. S. Alwar and Y. R. Nagaraja, *J. Adhesion* **7**, 279 (1976).
- [2] R. D. Adams, J. Coppendale and N. A. Peppiatt, *J. Strain Anal.* **13**, 1 (1978).
- [3] T. Wah, *Trans. ASME, J. Eng. Ind.* **95**, 174 (1973).
- [4] T. Sawa, A. Iwata and H. Ishikawa, *J. Adhesion* **29**, 258 (1986).
- [5] T. Sawa, K. Temma and H. Ishikawa, *J. Adhesion* **31**, 33 (1989).
- [6] T. Sawa, K. Temma and T. Nishigaya, *J. Adhesion Sci. Technol.* **9**, 215 (1995).
- [7] T. Sawa, Y. Nakano and K. Temma, *J. Adhesion* **24**, 1 (1987).
- [8] J.A. Harris and R.D. Adams, *Int. J. Adhesion and Adhesives* **4**,2 (1984).
- [9] M.Y.Tsai, D.W.Oplinger and J.Morton, *Int.J. Solids Structures.* **35**.12. (1998)
- [10] Sato C. *Int. J. Adhesion and Adhesives* **10**.1016 (2009).
- [11] A.E. Bogdanovich, I. Kizhakkethara, *Composites:Part B*, **30**.(1999)
- [12] Y. Suzuki, *Bull. JSME.*, **27**, 231 (1984).
- [13] Lubulin.J.L. and Greenwich, *J. Appl. Mech.*, **24**, 255 (1957).

- [14] THEIN WAH, Int. J. mech. Sci., **18**, 223 (1976).
- [15] THEIN WAH, Int. J. Solids Structures, **12**, 491 (1976).
- [16] David W. Adkins, Composites Science and Technology, **22**, 209 (1985).
- [17] Campilho.R.D.S.G., de Moura, M.F.S.F., Domingues, J.J.M.S., Int.J. Adhesion and Adhesives, **29**, 2 (2009).
- [18] Wang, Chun H, Gunnion, Andrew J, Composites Science and Technology. 68,1 (2008).
- [19] Gacoin, A, Objois, A, Assih.J, Delmas.Y, J. Adhesion, 84, 1, (2008).
- [20] Hilmy, I; Ashcroft, I A, Crocombe, A D, Key Engineering Materials. **385-387**, (2008).
- [21] Gacoin, A., Assih.J., Objois, A, Delmas.Y, J. Adhesion Science and Technology, **21**, 9 (2007).
- [22] Herszberg.I. Gunnion, A.J, Composite Structures, **75**, 1-4 (2006).
- [23] Objois. A, Assih. J, Troalen, J P, J. Adhesion. **81**, 9, (2005).

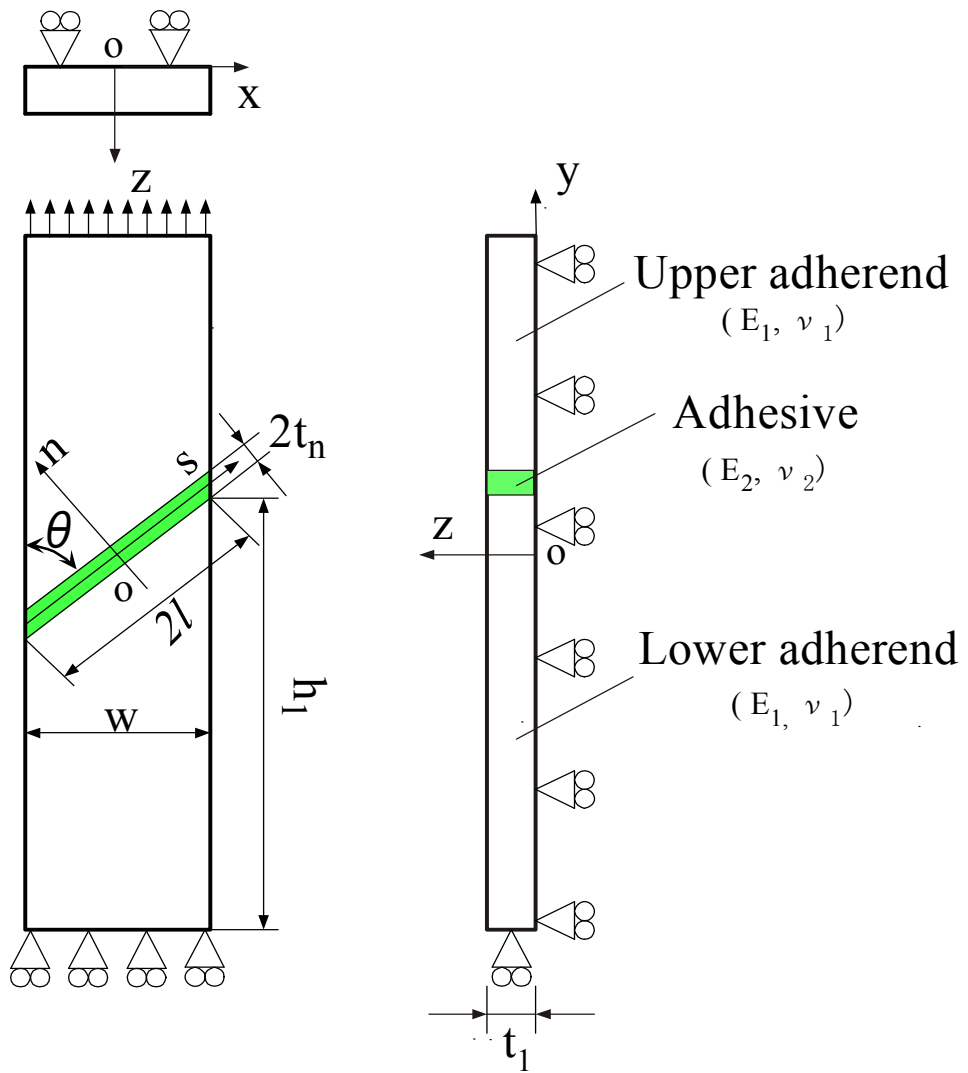
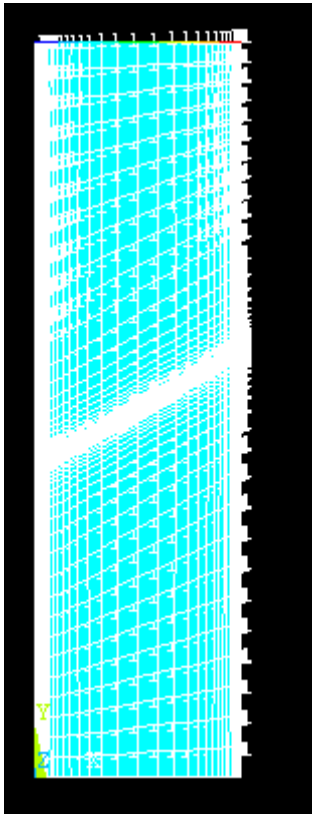
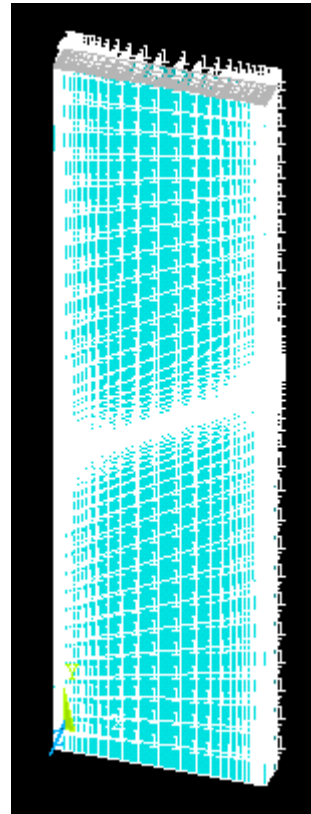


Fig.1 Model for 3-D FEM calculations



(a) Meshes in 2-D



(b) Meshes in 3-D

Fig. 2 An example of mesh division of scarf adhesive joints in 2-D (a) and 3-D FEM calculations (b)

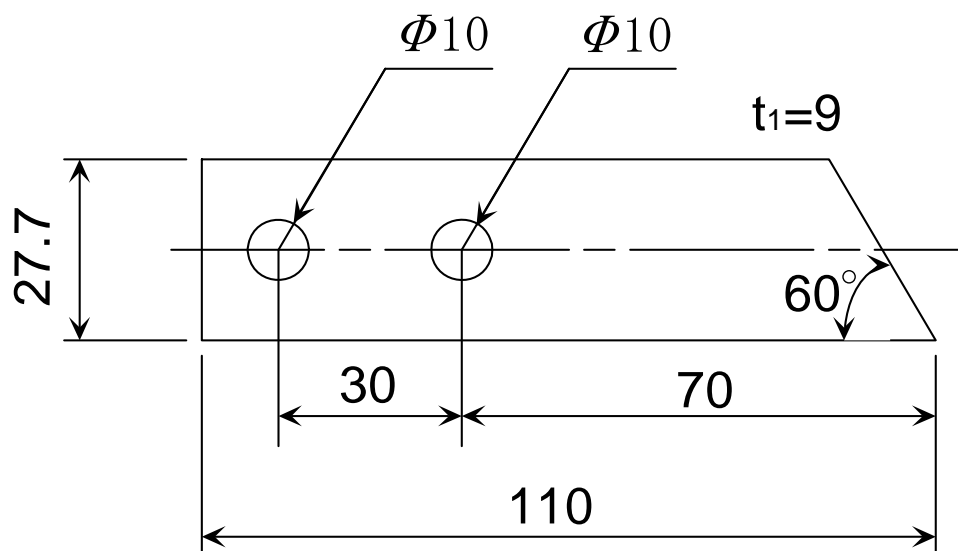


Fig. 3 Dimensions of adherends used in the experiments

(Unit: mm. thickness $t_1=9$ mm)

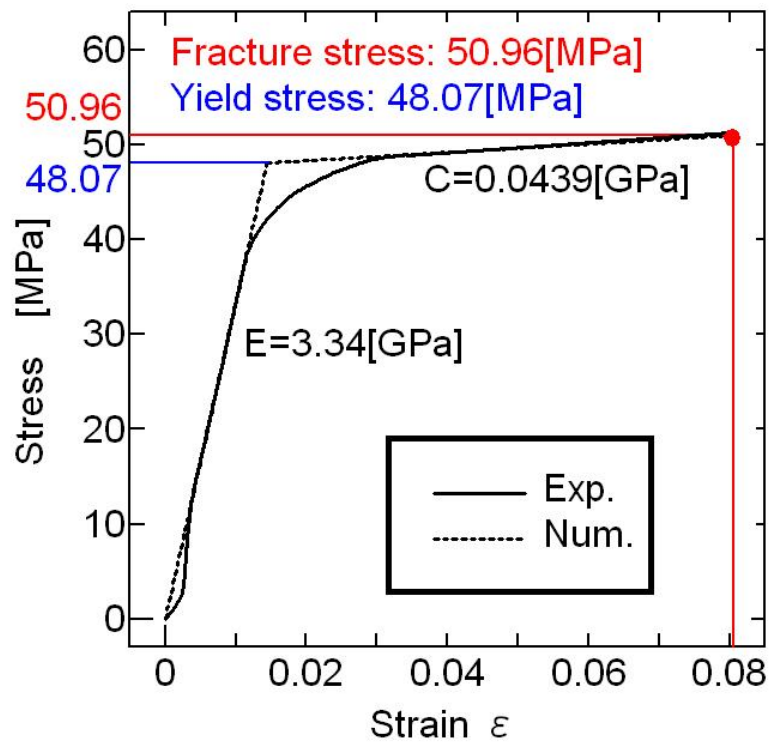


Fig.4 Measured Stress-strain relationship of the adhesive used in the present study (Solid line: measured, dotted line: FEM calculation)

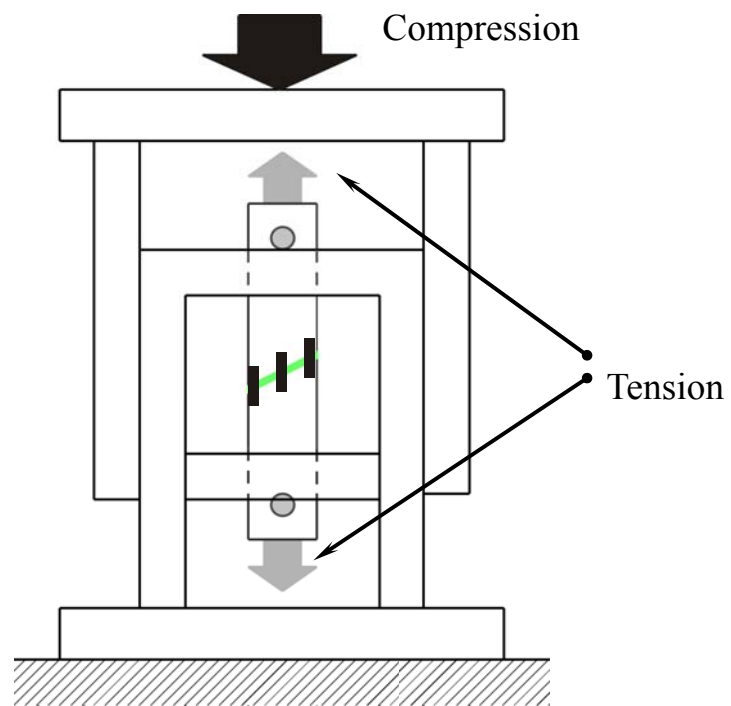
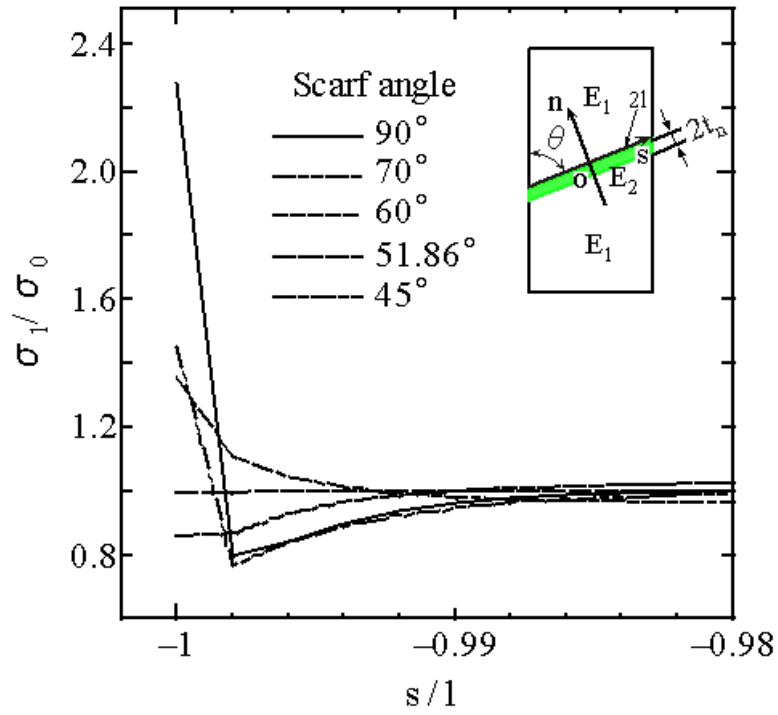
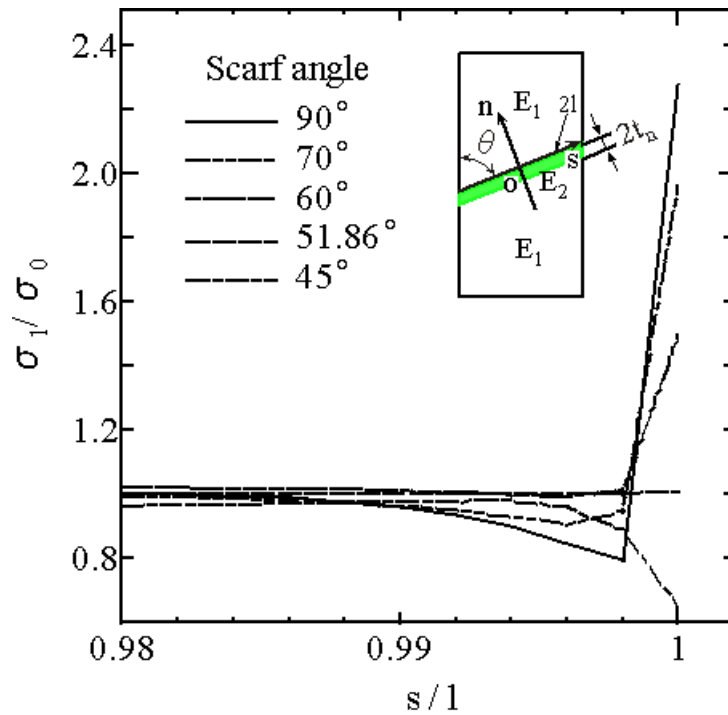


Fig. 5 Schematics of the experimental setup for measuring the strains and the joint strength under tensile loading (A compression was converted to a tension)



(a) Near the left edge of upper interface



(b) Near the right edge of upper interface

Fig.6 Effect of the scarf angles on the stress distributions using 2-D FEM (the plane strain state)

($E_1=209\text{GPa}$, $\nu_1=0.29$, $E_2=3.34\text{GPa}$, $\nu_2=0.38$, $2t_n=0.1\text{mm}$, $2l=32\text{mm}$)

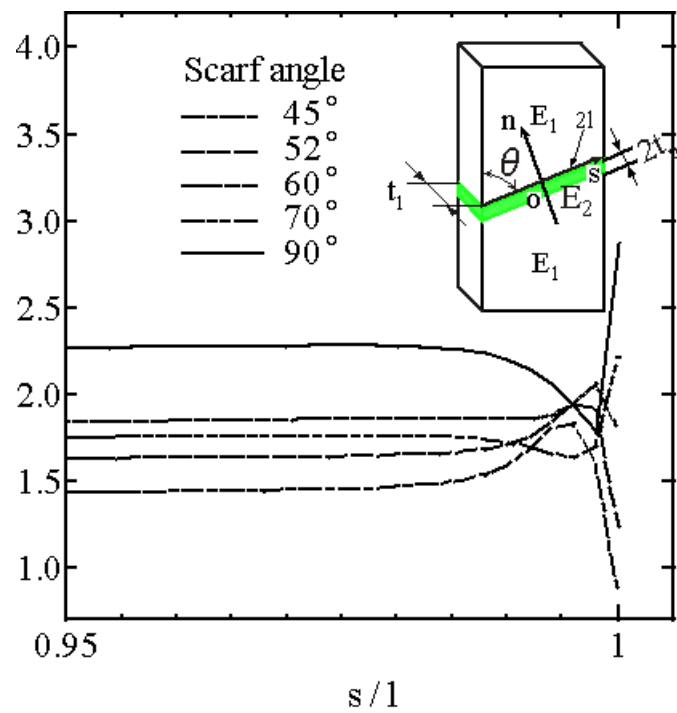
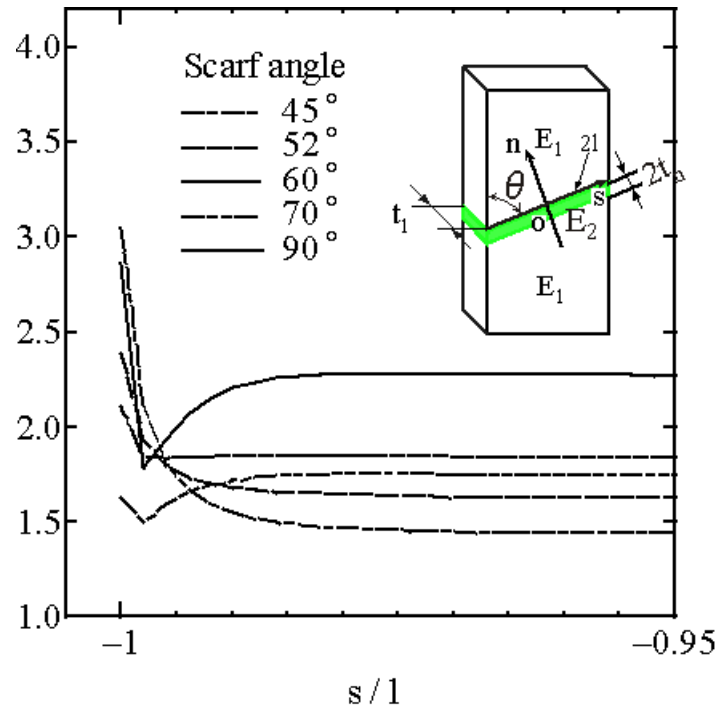


Fig.7 Effect of scarf angles on the stress distributions obtained from 3-D FEM calculations

($E_1=209\text{GPa}$, $\nu_1=0.29$, $E_2=3.34\text{GPa}$, $\nu_2=0.38$, $2t_n=0.1\text{mm}$, $2l=32\text{mm}$, $t_1=4.5\text{mm}$)

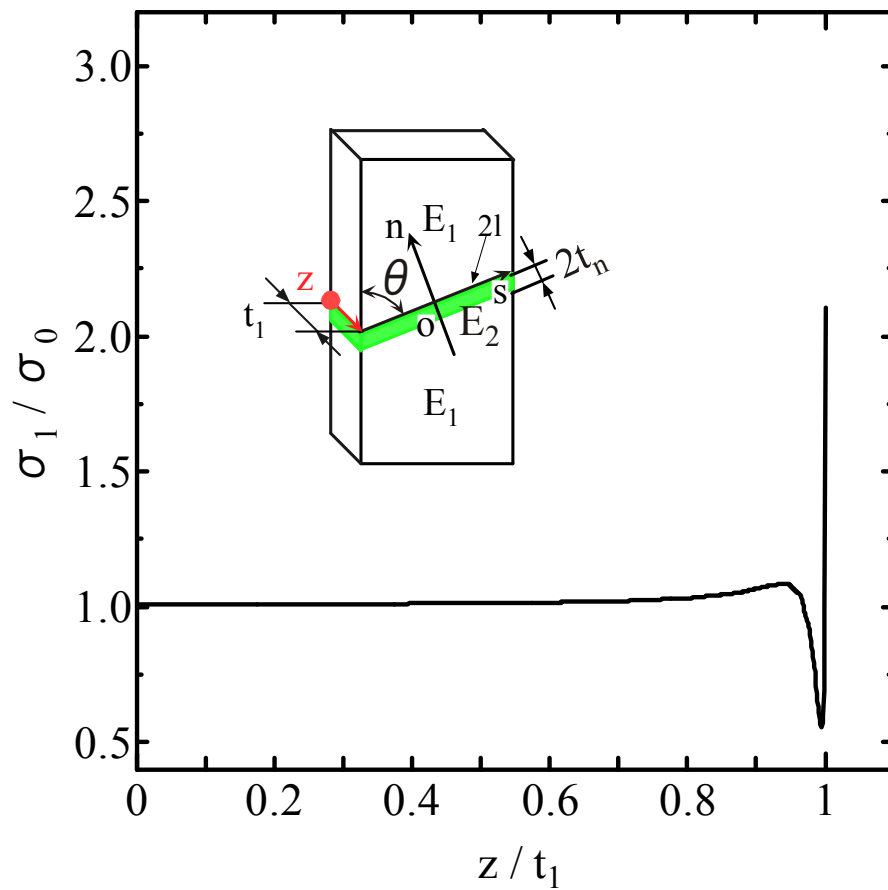


Fig.8 Normalized stress distribution obtained from 3-D FEM calculations at the interface ($s=-l, n=0$) in the adherend thickness direction ($E_1=209\text{GPa}, \nu_1=0.29, E_2=3.34\text{GPa}, \nu_2=0.38, \theta=60^\circ, 2t_n=0.1\text{mm}, 2l=32\text{mm}, t_1=4.5\text{mm}$)

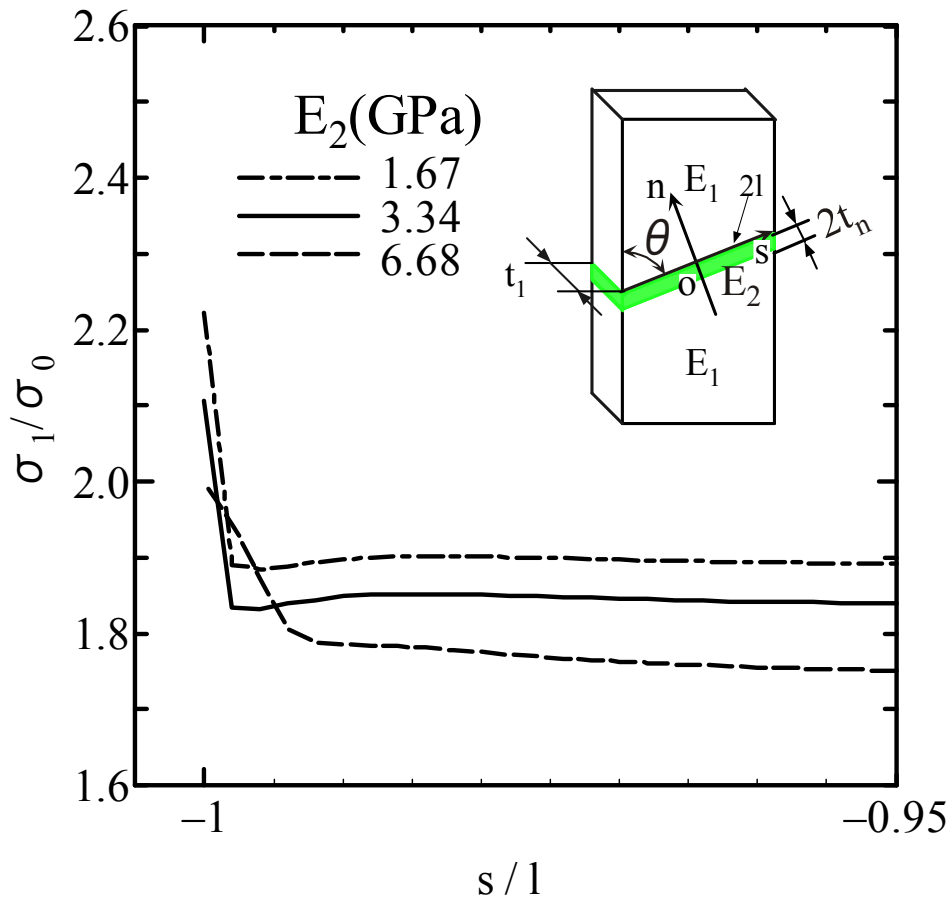


Fig.9 Effect of adhesive Young's modulus on the interface stress distributions near the left corner ($s/l=-1, z/t=1$) obtained from 3-D FEM calculations ($E_1=209\text{GPa}, \nu_1=0.29, \nu_2=0.38, \theta=60^\circ, 2t_n=0.1\text{mm}, 2l=32\text{mm}, t_1=4.5\text{mm}$)

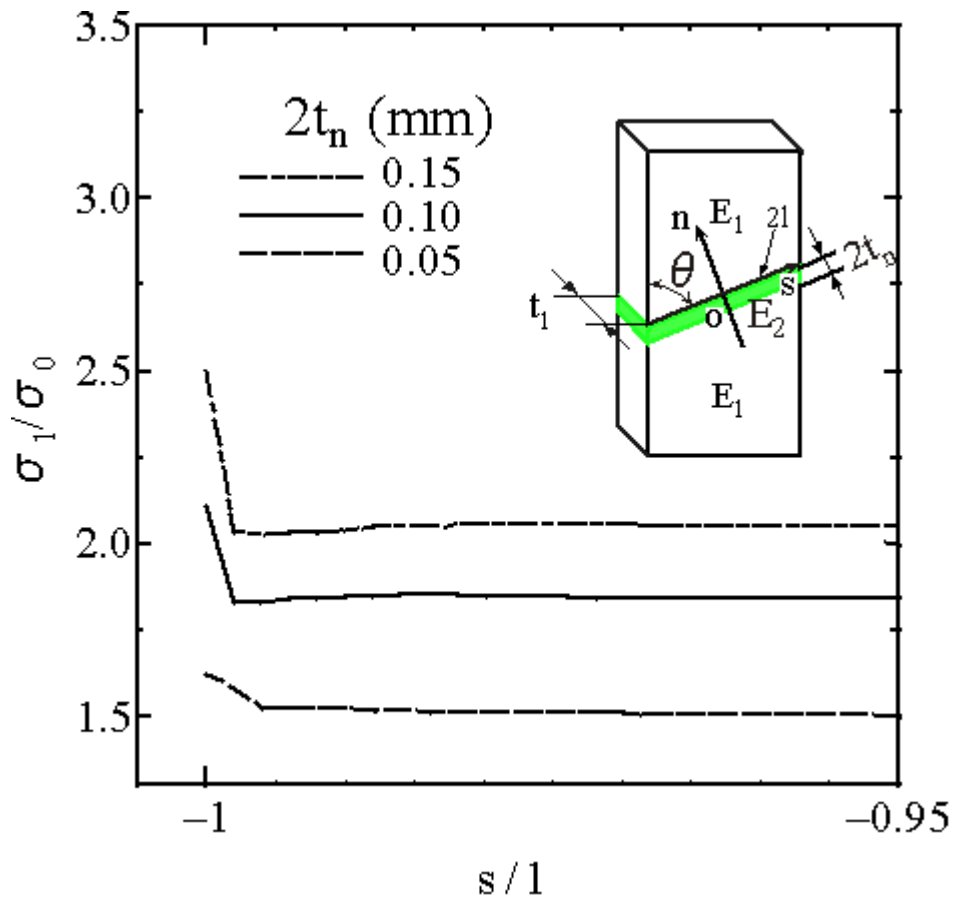


Fig.10 Effect of adhesive thickness on the interface stress distributions near the left corner ($s/l=-1$, $z/t=1$) obtained from 3-D FEM calculations ($E_1=209\text{GPa}$, $\nu_1=0.29$, $E_2=3.34\text{GPa}$, $\nu_2=0.38$, $\theta=60^\circ$, $2l=32\text{mm}$, $t_1=4.5\text{mm}$)

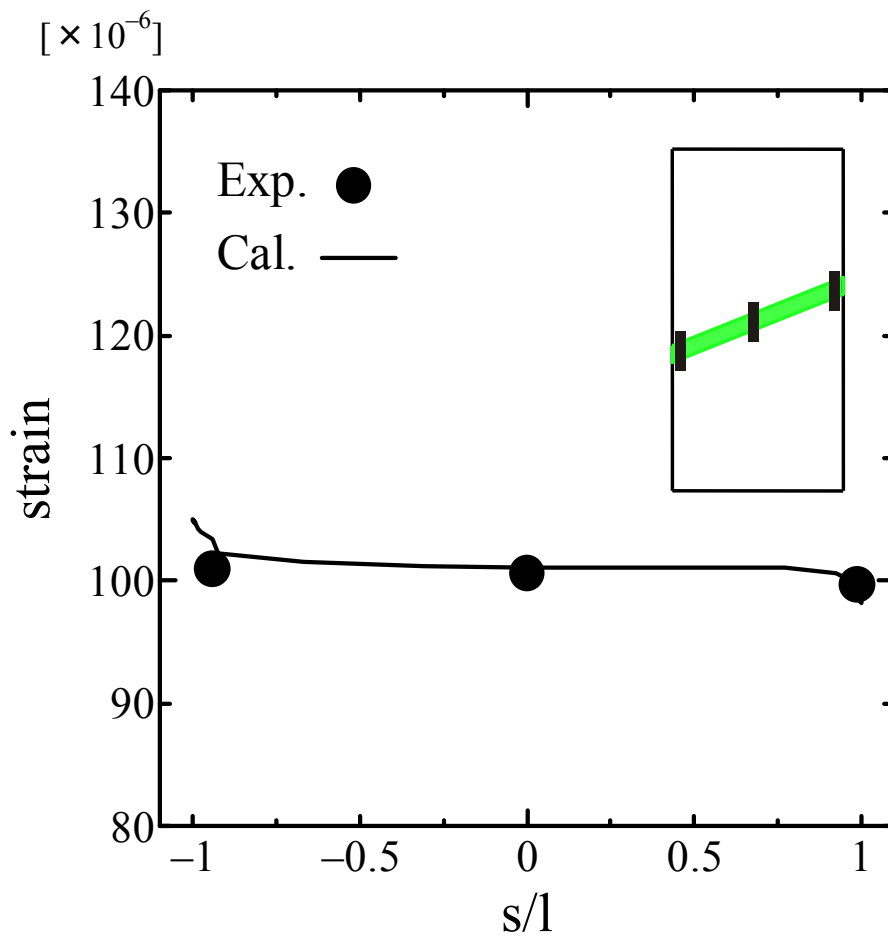


Fig.11 Comparison of the strain in the scarf adhesive joint between the 3-D FEM calculations and the experimental results ($E_1=209\text{GPa}$, $\nu_1=0.29$, $E_2=3.34\text{GPa}$, $\nu_2=0.38$, $\theta=60^\circ$)

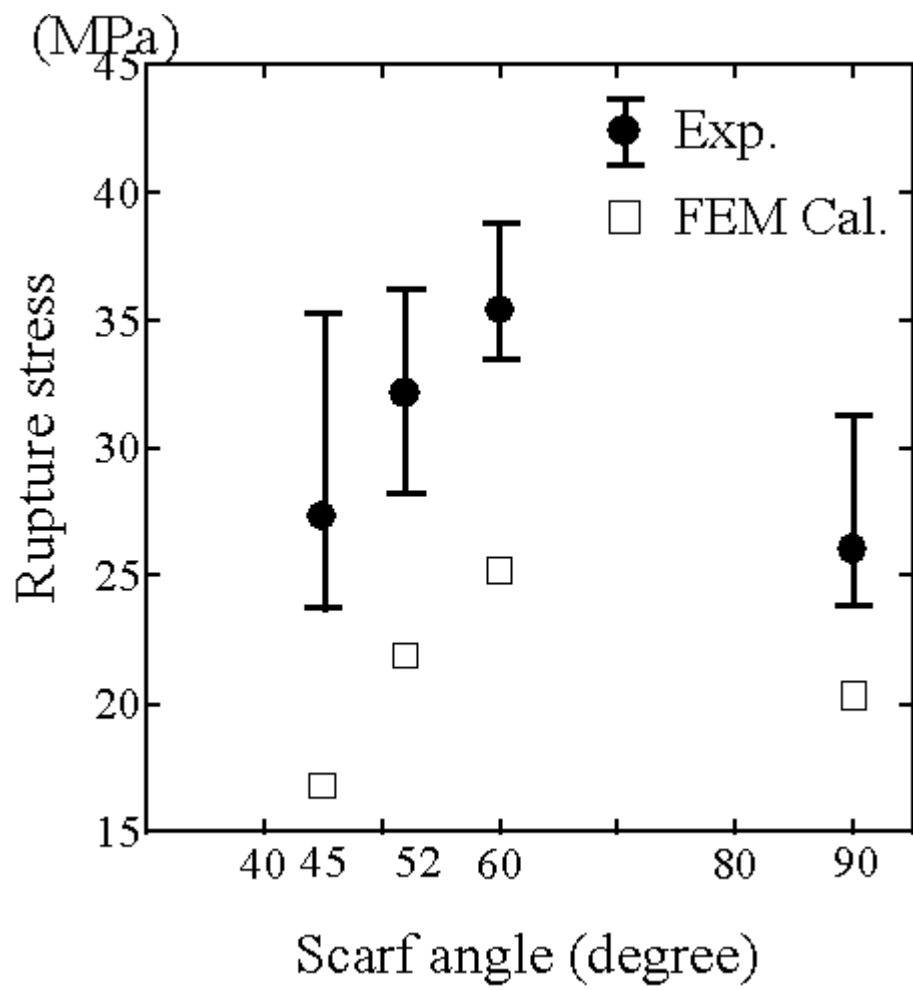


Fig.12 Effect of scarf angle on the strengths of scarf adhesive joints under static tensile loadings

Table 1 Width and scarf angle of the specimens

Scarf angle	Width(mm)
45°	22.6
52°	25.2
60°	27.7
90°	32